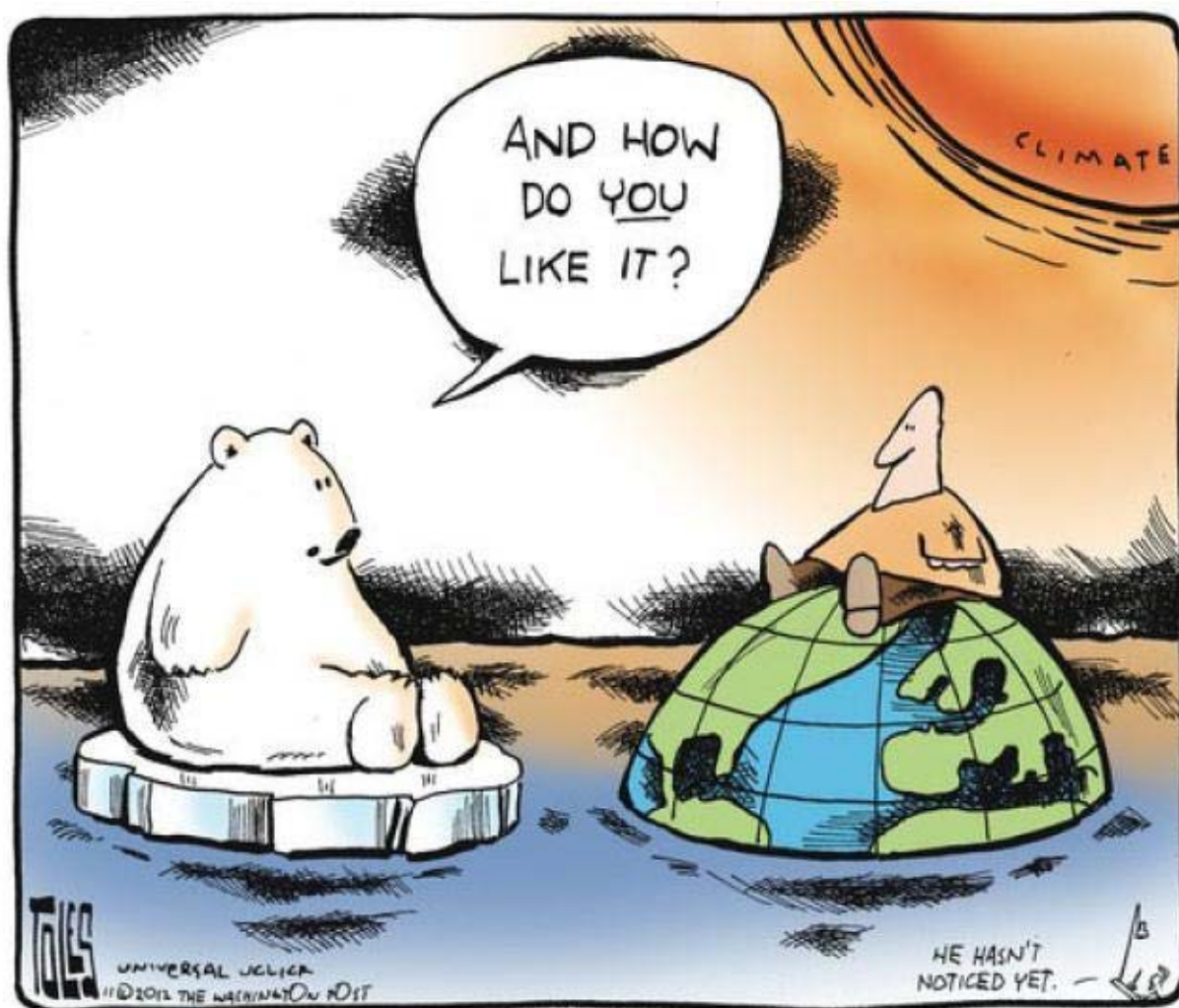


# FROM IPCC AR5 WKG I: THE ANTHROPOGENIC INFLUENCE ON THE CLIMATE CHANGE IS CLEAR

*Excerpts from IPCC AR5 by Toni Federico*

*Scientific Committee of Sustainable Development Foundation*



# SUMMARY

<b>Note from editor</b>	<b>3</b>
<b>A. Introduction</b>	<b>3</b>
<b>B. Observed Changes in the Climate System</b>	<b>3</b>
<b>C. Drivers of Climate Change</b>	<b>4</b>
<b>TS.3 (More on) Drivers of Climate Change</b>	<b>5</b>
TS.3.5 Radiative Forcing from Natural Drivers of Climate Change	7
TS.3.6 Synthesis of Forcings - Spatial and Temporal Evolution	9
TS.3.7 Climate Feedbacks	11
<b>D.3 Detection and Attribution of Climate Change</b>	<b>12</b>
Climate is Always Changing. How do we Determine the Causes of Observed Changes?	17
When Will Human Influences on Climate Become Obvious on Local Scales?	20
<b>Greenhouse Gas Variations and Past Climate Responses</b>	<b>23</b>
Observed Recent Climate Change in the Context of Interglacial Climate Variability	24
Pre-Industrial non-anthropogenic perspective on Radiative Forcing Factors	25
Atmospheric Concentrations of Carbon Dioxide, Methane and Nitrous Oxide from Ice Cores	26
May be the Sun the Major Driver of Recent Changes in Climate?	28
Temperature Variations During the Last 2000 Years	30
Past Interglacials Temperature Anomalies	32

*From combined evidence, it is virtually certain that human influence has warmed the global climate system. (IPCC AR5 WGI, ch. 10 pag. 931)*

## **Note from editor**

The materials, texts, graphs and images here edited are strictly identical to those of IPCC AR5 reports and summaries. Only the sequence is changed, under my complete responsibility, in order to achieve a straightforward evidence of the anthropogenic cause of current climate change. It is worth while to recall that IPCC does not produce climatic science research by itself, but only collects and displays all the results over the world from credited fonts after a very long and accurate process of documentation followed by discussions among the experts, and in some case even by votations.

## **A. Introduction<sup>1</sup>**

The Working Group I contribution to the IPCC's Fifth Assessment Report (AR5) considers new evidence of climate change based on many independent scientific analyses from observations of the climate system, paleoclimate archives, theoretical studies of climate processes and simulations using climate models. It builds upon the Working Group I contribution to the IPCC's Fourth Assessment Report (AR4), and incorporates subsequent new findings of research.

## **B. Observed Changes in the Climate System**

Observations of the climate system are based on direct measurements and remote sensing from satellites and other platforms. Global-scale observations from the instrumental era began in the mid-19th century for temperature and other variables, with more comprehensive and diverse sets of observations available for the period 1950 onwards. Paleoclimate reconstructions extend some records back hundreds to millions of years. Together, they provide a comprehensive view of the variability and long-term changes in the atmosphere, the ocean, the cryosphere, and the land surface.

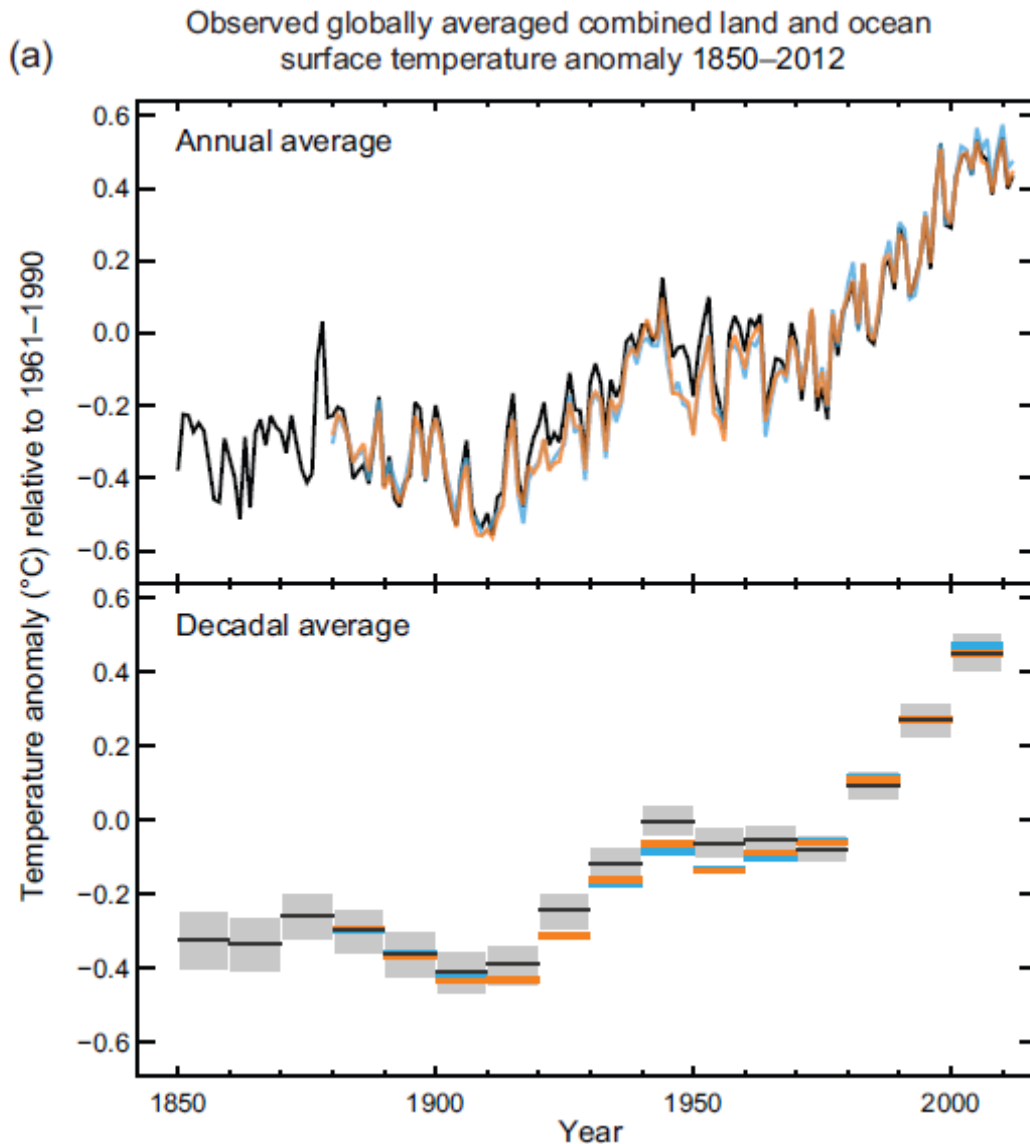
Warming of the climate system is unequivocal, and since the 1950s, many of the observed changes are unprecedented over decades to millennia. The

---

<sup>1</sup> Materials from: IPCC, 2013: *Summary for Policymakers*. In: *Climate Change 2013: The Physical Science Basis. Contribution of Working Group I to the Fifth Assessment Report of the Intergovernmental Panel on Climate Change* [Stocker, T.F., D. Qin, G.-K. Plattner, M. Tignor, S.K. Allen, J. Boschung, A. Nauels, Y. Xia, V. Bex and P.M. Midgley (eds.)]. Cambridge University Press, Cambridge, United Kingdom and New York, NY, USA.

atmosphere and ocean have warmed (Fig. SPM 1), the amounts of snow and ice have diminished, sea level has risen, and the concentrations of greenhouse gases have increased.

**Figure SPM.1 (a) Observed global mean combined land and ocean surface temperature anomalies, from 1850 to 2012 from three data sets. Top panel: annual mean values. Bottom panel: decadal mean values including the estimate of uncertainty for one dataset (black). Anomalies are relative to the mean of 1961–1990.**



## C. Drivers of Climate Change

Natural and anthropogenic substances and processes that alter the Earth's energy budget are drivers of climate change. Radiative forcing (RF)<sup>2</sup>

<sup>2</sup> The strength of drivers is quantified as Radiative Forcing (RF) in units watts per square metre ( $W m^{-2}$ ). RF is the change in energy flux caused by a driver, and is calculated at the tropopause or at the top of the atmosphere. In the traditional RF concept employed in previous IPCC reports all surface and tropospheric conditions are kept fixed. In calculations

quantifies the change in energy fluxes caused by changes in these drivers for 2011 relative to 1750. Positive RF leads to surface warming, negative RF leads to surface cooling. RF is estimated based on in-situ and remote observations, properties of greenhouse gases and aerosols, and calculations using numerical models representing observed processes. Some emitted compounds affect the atmospheric concentration of other substances. The RF can be reported based on the concentration changes of each substance. Alternatively, the emission-based RF of a compound can be reported, which provides a more direct link to human activities. It includes contributions from all substances affected by that emission. The total anthropogenic RF of the two approaches are identical when considering all drivers. Though both approaches are used in this Summary, emission-based RFs are emphasized.

Total radiative forcing is positive, and has led to an uptake of energy by the climate system. The largest contribution to total radiative forcing is caused by the increase in the atmospheric concentration of CO<sub>2</sub> since 1750.

### **TS.3 (More on) Drivers of Climate Change<sup>3</sup>**

Human activities have changed and continue to change the Earth's surface and atmospheric composition. Some of these changes have a direct or indirect impact on the energy balance of the Earth and are thus drivers of climate change. Radiative forcing (RF) is a measure of the net change in the energy balance of the Earth system in response to some external perturbation (see Box TS.2), with positive RF leading to a warming and negative RF to a cooling. The RF concept is valuable for comparing the influence on Global Mean Surface Temperature of most individual agents affecting the Earth's radiation balance. The quantitative values provided in AR5 are consistent with those in previous IPCC reports, though there have been some important revisions (Figure TS.6). Effective radiative forcing (ERF) is now used to quantify the impact of some forcing agents that involve rapid adjustments of components of the atmosphere and surface that are

---

of RF for well-mixed greenhouse gases and aerosols in this report, physical variables, except for the ocean and sea ice, are allowed to respond to perturbations with rapid adjustments. The resulting forcing is called Effective Radiative Forcing (ERF) in the underlying report. This change reflects the scientific progress from previous assessments and results in a better indication of the eventual temperature response for these drivers. For all drivers other than well-mixed greenhouse gases and aerosols, rapid adjustments are less well characterized and assumed to be small, and thus the traditional RF is used

<sup>3</sup> Approfondimenti sul tema del Radiative Forcing, trattato nel capitolo precedente, ricavati dal documento di Sintesi Tecnica: Stocker, T.F. et al. 2013, "Technical Summary. In: Climate Change 2013: The Physical Science Basis. Contribution of Working Group I to the Fifth Assessment Report of the Intergovernmental Panel on Climate Change", Cambridge University Press, Cambridge, United Kingdom and New York, NY, USA

assumed constant in the RF concept (see Box TS.2). RF and ERF are estimated from the change between 1750 and 2011, referred to as 'Industrial Era', if other time periods are not explicitly stated. Uncertainties are given associated with the best estimates of RF and ERF, with values representing the 5 to 95% (90%) confidence range (Fig. TS.7).

In addition to the global mean RF or ERF, the spatial distribution and temporal evolution of forcing, as well as climate feedbacks, play a role in determining the eventual impact of various drivers on climate. Land surface changes may also impact the local and regional climate through processes that are not radiative in nature.

**E**

### **Box TS.2 Radiative Forcing and Effective Radiative Forcing**

**E**

RF and ERF are used to quantify the change in the Earth's energy balance that occurs as a result of an externally imposed change. They are expressed in watts per square metre ( $W m^{-2}$ ). RF is defined in AR5, as in previous IPCC assessments, as the change in net downward flux (shortwave + longwave) at the tropopause after allowing for stratospheric temperatures to readjust to radiative equilibrium, while holding other state variables such as tropospheric temperatures, water vapour and cloud cover fixed at the unperturbed values.

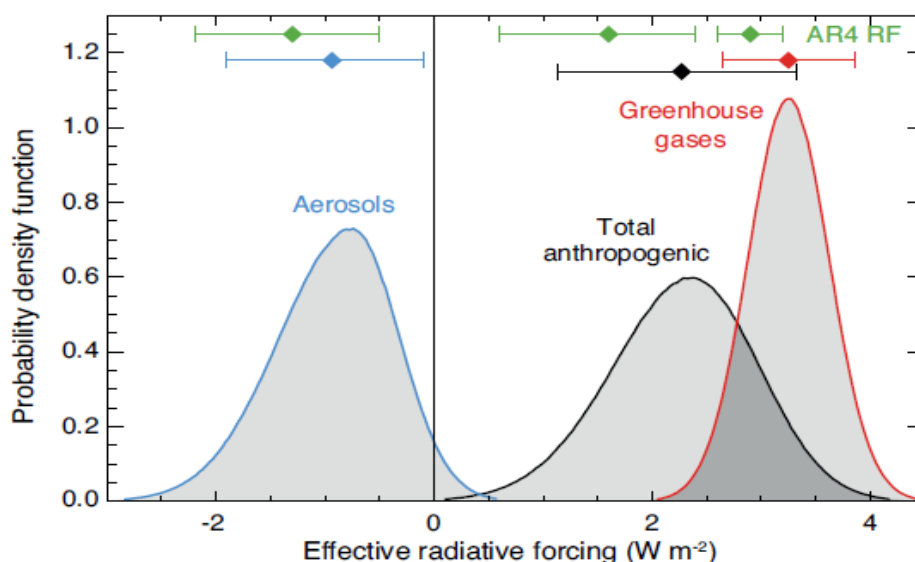
**E**

Although the RF concept has proved very valuable, improved understanding has shown that including rapid adjustments of the Earth's surface and troposphere can provide a better metric for quantifying the climate response. These rapid adjustments occur over a variety of time scales, but are relatively distinct from responses to GMST change. Aerosols in particular impact the atmosphere temperature profile and cloud properties on a time scale much shorter than adjustments of the ocean (even the upper layer) to forcings. The ERF concept defined in AR5 allows rapid adjustments to perturbations, for all variables except for GMST or ocean temperature and sea ice cover. The ERF and RF values are significantly different for the anthropogenic aerosols, owing to their influence on clouds and on snow or ice cover. For other components that drive the Earth's energy balance, such as GHGs, ERF and RF are fairly similar, and RF may have comparable utility given that it requires fewer computational resources to calculate and is not affected by meteorological variability and hence can better isolate small forcings. In cases where RF and ERF differ substantially, ERF has been shown to be a better indicator of the GMST response and is therefore emphasized in AR5.

**TS.3.5 Radiative Forcing from Natural Drivers of Climate Change**

Solar and volcanic forcings are the two dominant natural contributors to global climate change during the Industrial Era. Satellite observations of **total solar irradiance (TSI)** changes since 1978 show quasi-periodic cyclical variation with a period of roughly 11 years. Longer term forcing is typically estimated by comparison of solar minima (during which variability is least). This gives an RF change of  $-0.04$  [ $-0.08$  to  $0.00$ ]  $\text{W m}^{-2}$  between the most recent (2008) minimum and the 1986 minimum.

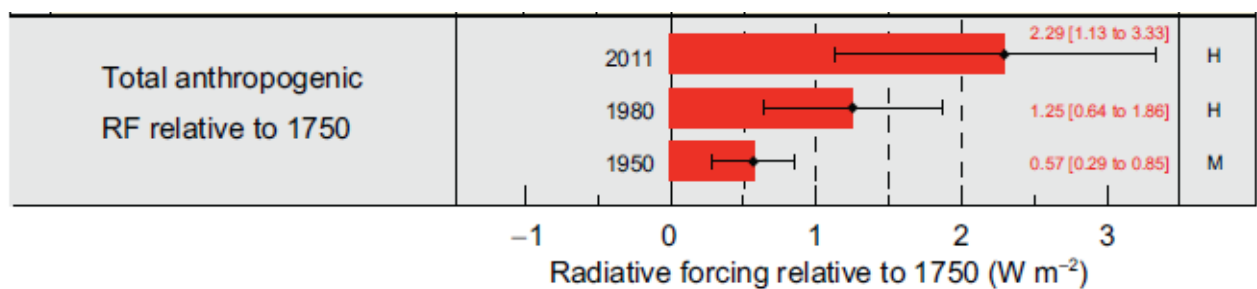
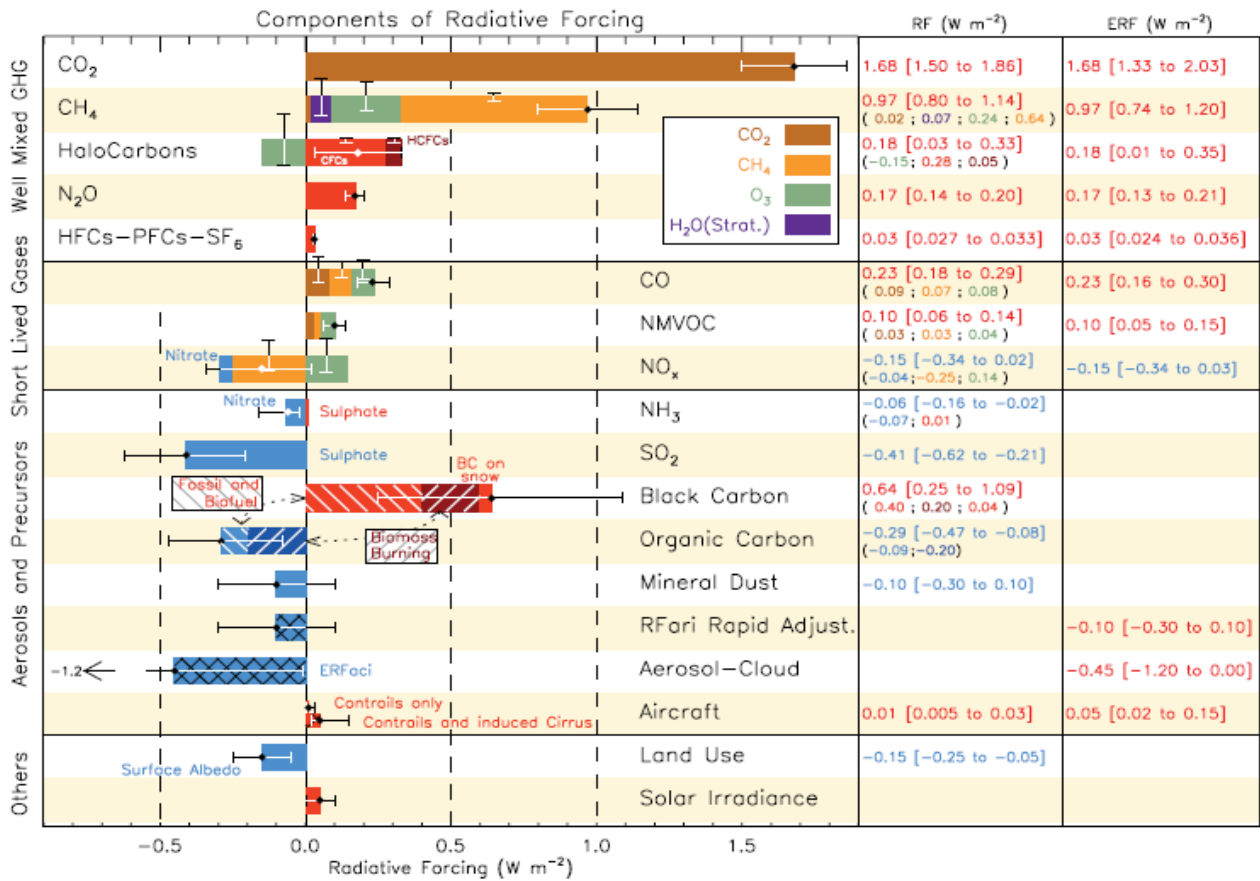
**Figure TS.6 (Bottom) Probability density functions (PDFs) for the ERF, for the aerosol, greenhouse gas (GHG) and total.** The green lines show the AR4 RF 90% confidence intervals and can be compared with the red, blue and black lines which show the AR5 ERF 90% confidence intervals (although RF and ERF differ, especially for aerosols). The ERF from surface albedo changes and combined contrails and contrail-induced cirrus is included in the total anthropogenic forcing, but not shown as a separate PDF. For some forcing mechanisms (ozone, land use, solar) the RF is assumed to be representative of the ERF.



Secular trends of TSI before the start of satellite observations rely on a number of indirect proxies. The best estimate of RF from TSI changes over the industrial era is  $0.05$  [ $0.00$  to  $0.10$ ]  $\text{W m}^{-2}$ , which includes greater RF up to around 1980 and then a small downward trend. This RF estimate is substantially smaller than the AR4 estimate due to the addition of the latest solar cycle and inconsistencies in how solar RF was estimated in earlier IPCC assessments. The recent solar minimum appears to have been unusually low and long-lasting and several projections indicate lower TSI for the forthcoming decades. However, current abilities to project solar irradiance are extremely limited so that there is very low confidence concerning future solar forcing. Nonetheless, **there is a high confidence that 21st century solar forcing will be much smaller than the projected increased forcing due to**

WMGHGs. Changes in solar activity affect the cosmic ray flux impinging upon the Earth's atmosphere, which has been hypothesized to affect climate through changes in cloudiness.

**Figure TS.7 + SPM.5 Radiative forcing (RF) of climate change during the Industrial Era shown by emitted components from 1750 to 2011.** The horizontal bars indicate the overall uncertainty, while the vertical bars are for the individual components (vertical bar lengths proportional to the relative uncertainty, with a total length equal to the bar width for a  $\pm 50\%$  uncertainty). Best estimates for the totals and individual components (from left to right) of the response are given in the right column. Values are RF except for the effective radiative forcing (ERF) due to aerosol-cloud interactions (ERFaci) and rapid adjustment associated with the RF due to aerosol-radiation interaction (RFari Rapid Adjust.). The ERF of contrails includes contrail induced cirrus. Combining ERFaci  $-0.45$  [ $-1.2$  to  $0.0$ ]  $Wm^{-2}$  and rapid adjustment of ari  $-0.1$  [ $-0.3$  to  $+0.1$ ]  $Wm^{-2}$  results in an integrated component of adjustment due to aerosols of  $-0.55$  [ $-1.33$  to  $-0.06$ ]  $Wm^{-2}$ . CFCs = chlorofluorocarbons, HCFCs = hydrochlorofluorocarbons, HFCs = hydrofluorocarbons, PFCs = perfluorocarbons, NMVOC = Non-Methane Volatile Organic Compounds, BC = black carbon.



The RF of stratospheric volcanic aerosols is now well understood and there is a large RF for a few years after major volcanic eruptions. Although volcanic eruptions inject both mineral particles and sulphate aerosol precursors into the atmosphere, it is the latter, because of their small size and long lifetimes, that are responsible for RF important for climate. The emissions of CO<sub>2</sub> from volcanic eruptions are at least 100 times smaller than anthropogenic emissions, and inconsequential for climate on century time scales. Large tropical volcanic eruptions have played an important role in driving annual to decadal scale climate change during the Industrial Era owing to their sometimes very large negative RF. There has not been any major volcanic eruption since Mt Pinatubo in 1991, which caused a 1-year RF of about  $-3.0 \text{ W m}^{-2}$ , but several smaller eruptions have caused an RF averaged over the years 2008–2011 of  $-0.11$  [ $-0.15$  to  $-0.08$ ]  $\text{W m}^{-2}$ , twice as strong in magnitude compared to the 1999–2002 average. The smaller eruptions have led to better understanding of the dependence of RF on the amount of material from high-latitude injections as well as the time of the year when they take place.

### ***TS.3.6 Synthesis of Forcings - Spatial and Temporal Evolution***

A synthesis of the Industrial Era forcing finds that **among the forcing agents, there is a very high confidence only for the Well Mixed GHG RF.**

The time evolution of the total anthropogenic RF shows a nearly continuous increase from 1750, primarily since about 1860. The total anthropogenic RF increase rate since 1960 has been much greater than during earlier Industrial Era periods, driven primarily by the continuous increase in most WMGHG concentrations. There is still low agreement on the time evolution of the total aerosol ERF, which is the primary factor for the uncertainty in the total anthropogenic forcing. The fractional uncertainty in the total anthropogenic forcing decreases gradually after 1950 owing to the smaller offset of positive WMGHG forcing by negative aerosol forcing.

There is **robust evidence and high agreement that natural forcing is a small fraction of the WMGHG forcing.** Natural forcing changes over the last 15 years have likely offset a substantial fraction (at least 30%) of the anthropogenic forcing increase during this period. **Forcing by CO<sub>2</sub> is the largest single contributor to the total forcing during the Industrial Era and from 1980–2011.** Compared to the entire Industrial Era, the dominance of CO<sub>2</sub> forcing is larger for the 1980–2011 change with respect to other WMGHGs, and there is high confidence that the offset from aerosol forcing

to WMGHG forcing during this period was much smaller than over the 1950–1980 period.

Forcing can also be attributed to emissions rather than to the resulting concentration changes (Figure TS.7). Carbon dioxide is the largest single contributor to historical RF from either the perspective of changes in the atmospheric concentration of CO<sub>2</sub> or the impact of changes in net emissions of CO<sub>2</sub>. The relative importance of other forcing agents can vary markedly with the perspective chosen, however. In particular, CH<sub>4</sub> emissions have a much larger forcing (about 1.0 W m<sup>-2</sup> over the Industrial Era) than CH<sub>4</sub> concentration increases (about 0.5 W m<sup>-2</sup>) due to several indirect effects through atmospheric chemistry. In addition, carbon monoxide emissions are virtually certain to cause a positive forcing, while emissions of reactive nitrogen oxides likely cause a net negative forcing but uncertainties are large.

Emissions of ozone-depleting halocarbons very likely cause a net positive forcing as their direct radiative effect is larger than the impact of the stratospheric ozone depletion that they induce. Emissions of SO<sub>2</sub>, organic carbon and ammonia cause a negative forcing, while emissions of black carbon lead to positive forcing via aerosol–radiation interactions. Note that mineral dust forcing may include a natural component or a climate feedback effect.

Although the WMGHGs show a spatially fairly homogeneous forcing, other agents such as aerosols, ozone and land use changes are highly heterogeneous spatially. RF<sub>ari</sub> showed maximum negative values over eastern North America and Europe during the early 20th century, with large negative values extending to East and Southeast Asia, South America and central Africa by 1980. Since then, however, the magnitude has decreased over eastern North America and Europe due to pollution control, and the peak negative forcing has shifted to South and East Asia primarily as a result of economic growth and the resulting increase in emissions in those areas. Total aerosol ERF shows similar behaviour for locations with maximum negative forcing, but also shows substantial positive forcing over some deserts and the Arctic. In contrast, the global mean whole atmosphere ozone forcing increased throughout the 20<sup>th</sup> century, and has peak positive amplitudes around 15°N to 30°N but negative values over Antarctica.

Negative land use forcing by albedo changes has been strongest in industrialized and biomass burning regions. The inhomogeneous nature of

these forcings can cause them to have a substantially larger influence on the hydrologic cycle than an equivalent global mean homogeneous forcing.

### ***TS.3.7 Climate Feedbacks***

Feedbacks will also play an important role in determining future climate change. Indeed, climate change may induce modification in the water, carbon and other biogeochemical cycles which may reinforce (positive feedback) or dampen (negative feedback) the expected temperature increase.

Snow and ice albedo feedbacks are known to be positive. The combined water vapour and lapse rate feedback is extremely likely to be positive and now fairly well quantified, while cloud feedbacks continue to have larger uncertainties. In addition, the new CMIP5 model consistently estimate a positive carbon-cycle feedback, that is, reduced natural CO<sub>2</sub> sinks in response to future climate change. In particular, carbon-cycle feedbacks in the oceans are positive. Carbon sinks in tropical land ecosystems are less consistent, and may be susceptible to climate change via processes such as drought and fire that are sometimes not yet fully represented.

Models and ecosystem warming experiments show high agreement that wetland CH<sub>4</sub> emissions will increase per unit area in a warmer climate, but wetland areal extent may increase or decrease depending on regional changes in temperature and precipitation affecting wetland hydrology, so that there is low confidence in quantitative projections of wetland CH<sub>4</sub> emissions.

Reservoirs of carbon in hydrates and permafrost are very large, and thus could potentially act as very powerful feedbacks. Although poorly constrained, the 21<sup>st</sup> century global release of CH<sub>4</sub> from hydrates to the atmosphere is likely to be low due to the under-saturated state of the ocean, long ventilation time of the ocean and slow propagation of warming through the seafloor. There is high confidence that release of carbon from thawing permafrost provides a positive feedback, but there is low confidence in quantitative projections of its strength.

Aerosol-climate feedbacks occur mainly through changes in the source strength of natural aerosols or changes in the sink efficiency of natural and anthropogenic aerosols; a limited number of studies have assessed the magnitude of this feedback to be small. There is medium confidence for a weak feedback (of uncertain sign) involving dimethylsulphide, cloud

condensation nuclei and cloud albedo due to a weak sensitivity of cloud condensation nuclei population to changes in dimethylsulphide emissions.

### **D.3 Detection and Attribution of Climate Change**

Human influence has been detected in warming of the atmosphere and the ocean, in changes in the global water cycle, in reductions in snow and ice, in global mean sea level rise, and in changes in some climate extremes. *This evidence for human influence has grown since AR4. It is extremely likely that human influence has been the dominant cause of the observed warming since the mid-20th century.*

It is extremely likely that more than half of the observed increase in global average surface temperature from 1951 to 2010 was caused by the anthropogenic increase in greenhouse gas concentrations and other anthropogenic forcings together. The best estimate of the human-induced contribution to warming is similar to the observed warming over this period.

Greenhouse gases contributed a global mean surface warming likely to be in the range of 0.5°C to 1.3°C over the period 1951 to 2010, with the contributions from other anthropogenic forcings, including the cooling effect of aerosols, likely to be in the range of –0.6°C to 0.1°C. The contribution from natural forcings is likely to be in the range of –0.1°C to 0.1°C, and from natural internal variability is likely to be in the range of –0.1°C to 0.1°C. Together these assessed contributions are consistent with the observed warming of approximately 0.6°C to 0.7°C over this period. It is very likely that anthropogenic influence, particularly greenhouse gases and stratospheric ozone depletion, has led to a detectable observed pattern of tropospheric warming and a corresponding cooling in the lower stratosphere since 1961.

It is very likely that anthropogenic forcings have made a substantial contribution to increases in global upper ocean heat content (0–700 m) observed since the 1970s

It is likely that anthropogenic influences have affected the global water cycle since 1960. Anthropogenic influences have contributed to observed increases in atmospheric moisture content in the atmosphere, to global-scale changes in precipitation patterns over land, to intensification of heavy precipitation over land regions where data are sufficient, and to changes in surface and sub-surface ocean salinity (very likely).

There has been further strengthening of the evidence for human influence on temperature extremes. It is now very likely that human influence has

contributed to observed global scale changes in the frequency and intensity of daily temperature extremes since the mid-20th century, and likely that human influence has more than doubled the probability of occurrence of heat waves in some locations.

Anthropogenic influences have very likely contributed to Arctic sea ice loss since 1979.

Anthropogenic influences likely contributed to the retreat of glaciers since the 1960s and to the increased surface mass loss of the Greenland ice sheet since 1993.

It is likely that there has been an anthropogenic contribution to observed reductions in Northern Hemisphere spring snow cover since 1970.

It is very likely that there is a substantial anthropogenic contribution to the global mean sea level rise since the 1970s. This is based on the high confidence in an anthropogenic influence on the two largest contributions to sea level rise, that is thermal expansion and glacier mass loss.

There is high confidence that changes in total solar irradiance have not contributed to the increase in global mean surface temperature over the period 1986 to 2008, based on direct satellite measurements of total solar irradiance. There is medium confidence that the 11-year cycle of solar variability influences decadal climate fluctuations in some regions. No robust association between changes in cosmic rays and cloudiness has been identified.

## **10. (More on) Detection and Attribution of Climate Change<sup>4</sup>**

Evidence of a human influence on climate has grown stronger over the period of the four previous assessment reports of the IPCC. There was little observational evidence for a detectable human influence on climate at the time of the First IPCC Assessment Report. By the time of the second report there was sufficient additional evidence for it to conclude that 'the balance of evidence suggests a discernible human influence on global climate'. The Third Assessment Report found that a distinct greenhouse gas (GHG) signal was robustly detected in the observed temperature record and that 'most of

---

<sup>4</sup> The Chapter 10 of the full AR5 WGI Report allows us to go deep in the attribution of climate changes. The reference is: IPCC, 2013, "Climate Change 2013: The Physical Science Basis. Contribution of Working Group I to the Fifth Assessment Report of the Intergovernmental Panel on Climate Change", Cambridge University Press, Cambridge, United Kingdom and New York, NY, USA, 1535 pp

the observed warming over the last fifty years is likely to have been due to the increase in greenhouse gas concentrations’.

With the additional evidence available by the time of the Fourth Assessment Report, the conclusions were further strengthened. This evidence included a wider range of observational data, a greater variety of more sophisticated climate models including improved representations of forcings and processes and a wider variety of analysis techniques. This enabled the AR4 report to conclude that ‘most of the observed increase in global average temperatures since the mid-20th century is very likely due to the observed increase in anthropogenic greenhouse gas concentrations’. The AR4 also concluded that ‘discernible human influences now extend to other aspects of climate, including ocean warming, continental-average temperatures, temperature extremes and wind patterns’.

The evidence has grown since the Fourth Assessment Report that widespread changes observed in the climate system since the 1950s are attributable to anthropogenic influences. This evidence is documented in the sections of chapter 10 of the Full Report AR5 WGI, including for near surface temperatures, free atmosphere temperatures, atmospheric moisture content, precipitation over land, ocean heat content, ocean salinity, sea level, Arctic sea ice, climate extremes and evidence from the last millenium paleoclimate. These results strengthen the conclusion that human influence on climate has played the dominant role in observed warming since the 1950s. However, the approach taken so far in the chapter has been to examine each aspect of the climate system - the atmosphere, oceans, cryosphere, extremes, and from paleoclimate archives - separately in each section and sub-section. In the following we look across the whole climate system to assess the extent that a consistent picture emerges across sub-systems and climate variables.

A combined analysis of near-surface temperature from weather stations and free atmosphere temperatures from radiosondes detected an anthropogenic influence on the joint changes in temperatures near the surface and aloft. In a Bayesian application of detection and attribution surface temperature, diurnal temperature range and precipitation were combined into a single analysis and showed strong net evidence for detection of anthropogenic forcings.

To demonstrate how observed changes across the climate system can be understood in terms of natural and anthropogenic causes observed and modelled changes in the atmosphere, ocean and cryosphere were compared.

The instrumental records associated with each element of the climate system are generally independent, and consequently joint interpretations across observations from the main components of the climate system increases the confidence to higher levels than from any single study or component of the climate system. The ability of climate models to replicate observed changes (to within internal variability) across a wide suite of climate indicators also builds confidence in the capacity of the models to simulate the Earth's climate.

The coherence of observed changes for with climate model simulations that include anthropogenic and natural forcing is remarkable. Surface temperatures over land, SSTs and ocean heat content changes show emerging anthropogenic and natural signals with a clear separation between the observed changes and the alternative hypothesis of just natural variations. These signals appear not just in the global means, but also at continental and ocean basin scales in these variables. Sea ice emerges strongly from the range expected from natural variability for the Arctic and Antarctica remains broadly within the range of natural variability consistent with expectations from model simulations including anthropogenic forcings.

From up in the stratosphere, down through the troposphere to the surface of the Earth and into the depths of the oceans there are detectable signals of change [such that the assessed likelihood of a detectable, and often quantifiable, human contribution ranges from likely to extremely likely for many climate variables](#). Indeed to successfully describe the observed warming trends in the atmosphere, ocean and at the surface over the past 50 years, contributions from both anthropogenic and natural forcings are required. This is consistent with anthropogenic forcings warming the surface of the Earth, troposphere and oceans superimposed with cooling events caused by the three large explosive volcanic eruptions since the 1960's. These two effects (anthropogenic warming and volcanic eruptions) cause much of the observed response. Both natural and anthropogenic forcings are required to understand fully the variability of the Earth system during the past 50 years.

Water in the free atmosphere is expected to increase, as a consequence of warming of the atmosphere, and atmospheric circulation controls the global distribution of precipitation and evaporation. Simulations show that GHGs increase moisture in the atmosphere and change its transport in such a way as to produce patterns of precipitation and evaporation that are quite distinct from the observed patterns of warming. Our assessment shows that anthropogenic forcings have contributed to observed increases in moisture

content in the atmosphere, to global scale changes in precipitation patterns over land, to a global scale intensification of heavy precipitation in land regions where there observational coverage is sufficient to make an assessment, and to changes in surface and sub-surface ocean salinity. Combining evidence from both atmosphere and ocean that systematic changes in precipitation over land and ocean salinity can be attributed to human influence supports an assessment that it is likely that human influence has affected the global water cycle since 1960.

Warming of the atmosphere and the oceans affects the cryosphere, and in the case of snow and sea ice warming leads to positive feedbacks that amplify the warming response in the atmosphere and oceans. Retreat of mountain glaciers has been observed with an anthropogenic influence detected, Greenland ice sheet has melted at the edges and accumulating snow at the higher elevations is consistent with GHG warming supporting an assessment for an anthropogenic influence on the negative surface mass balance of Greenland's ice sheet. Our level of scientific understanding is still too low to provide a quantifiable explanation of the observed mass loss of the Antarctic ice sheet. Sea ice in the Arctic is decreasing rapidly and the changes now exceed internal variability and with an anthropogenic contribution detected. Antarctic sea ice extent has grown overall over the last 30 years but there is low scientific understanding of the spatial variability and changes in Antarctic sea ice extent.

Anthropogenic forcing has also affected temperature on continental scales, with human influences having made a substantial contribution to warming in each of the inhabited continents, and having contributed to the very substantial Arctic warming over the past 50 years, while because of large observational uncertainties there is low confidence in attribution of warming averaged over available stations over Antarctica.

There is also evidence that anthropogenic forcings have contributed to temperature change in many sub-continental regions and that anthropogenic forcings have contributed to the observed changes in the frequency and intensity of daily temperature extremes on the global scale since the mid-20th century. Furthermore there is evidence that human influence has substantially increased the probability of occurrence of heat waves in some locations.

An analysis of these results shows that there is high confidence in attributing many aspects of changes in the climate system to human influence including from atmospheric measurements of temperature.

Synthesizing the results shows that the combined evidence from across the climate system increases the level of confidence in the attribution of observed climate change to human influence and reduces the uncertainties associated with assessments based on a single variable.

**From this combined evidence, it is virtually certain that human influence has warmed the global climate system.**

*Climate is Always Changing. How do we Determine the Causes of Observed Changes?*

The causes of observed long-term changes in climate (on time scales longer than a decade) are assessed by determining whether the expected 'fingerprints' of different causes of climate change are present in the historical record. These fingerprints are derived from computer model simulations of the different patterns of climate change caused by individual climate forcings. On multi-decade time scales, these forcings include processes such as greenhouse gas increases or changes in solar brightness. By comparing the simulated fingerprint patterns with observed climate changes, we can determine whether observed changes are best explained by those fingerprint patterns, or by natural variability, which occurs without any forcing.

The fingerprint of human-caused greenhouse gas increases is clearly apparent in the pattern of observed 20th century climate change. The observed change cannot be otherwise explained by the fingerprints of natural forcings or natural variability simulated by climate models. Attribution studies therefore support the conclusion that 'it is extremely likely that human activities have caused more than half of the observed increase in global mean surface temperatures from 1951 to 2010'.

The Earth's climate is always changing, and that can occur for many reasons. To determine the principal causes of observed changes, we must first ascertain whether an observed change in climate is different from other fluctuations that occur without any forcing at all. Climate variability without forcing—called **internal variability**—is the consequence of processes within the climate system. Large-scale oceanic variability, such as El Niño-Southern Oscillation (ENSO) fluctuations in the Pacific Ocean, is the dominant source of internal climate variability on decadal to centennial time scales.

Climate change can also result from natural forcings external to the climate system, such as volcanic eruptions, or changes in the brightness of the sun.

Forcings such as these are responsible for the huge changes in climate that are clearly documented in the geological record. Human-caused forcings include greenhouse gas emissions or atmospheric particulate pollution. Any of these forcings, natural or human caused, could affect internal variability as well as causing a change in average climate. [Attribution studies attempt to determine the causes of a detected change in observed climate.](#) Over the past century we know that global average temperature has increased, so if the observed change is forced then the principal forcing must be one that causes warming, not cooling.

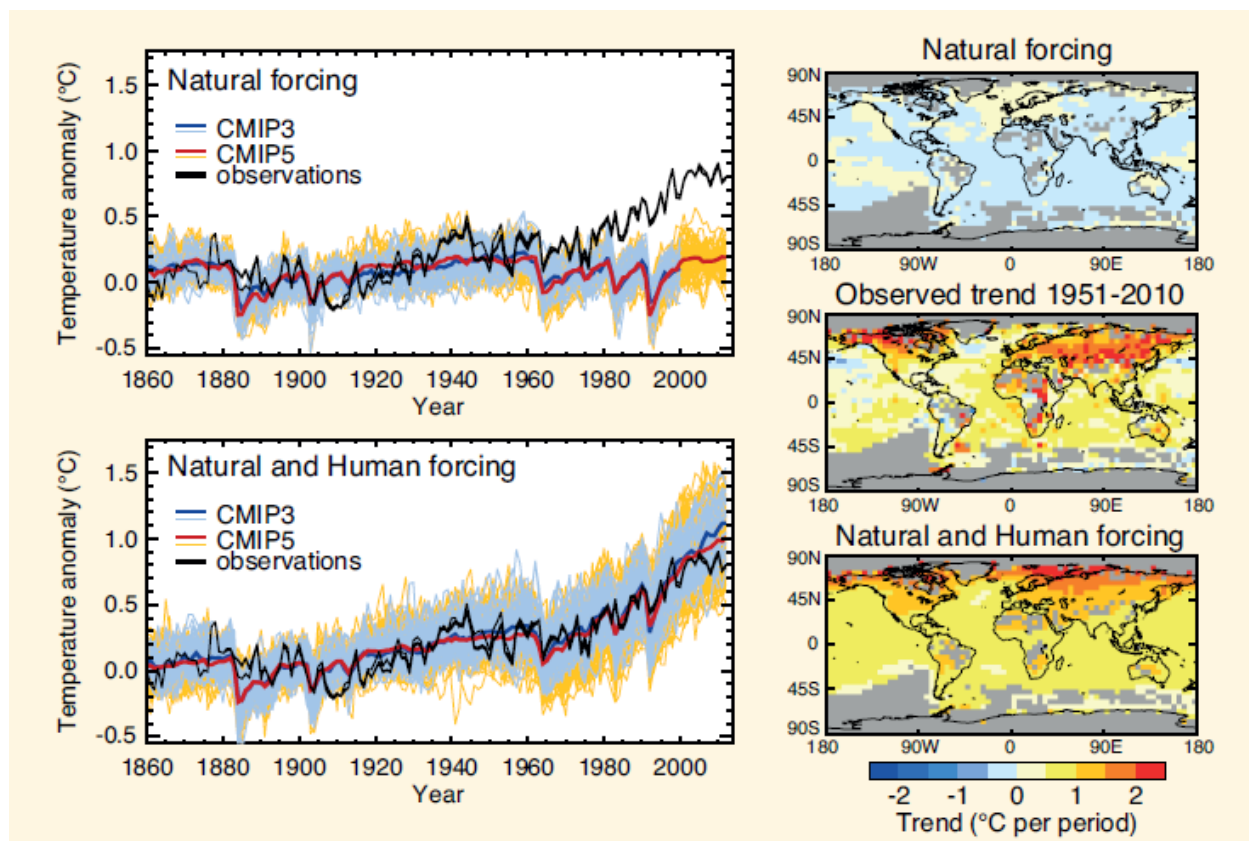
Formal climate change attribution studies are carried out using controlled experiments with climate models. The model-simulated responses to specific climate forcings are often called the fingerprints of those forcings. A climate model must reliably simulate the fingerprint patterns associated with individual forcings, as well as the patterns of unforced internal variability, in order to yield a meaningful climate change attribution assessment. No model can perfectly reproduce all features of climate, but many detailed studies indicate that simulations using current models are indeed sufficiently reliable to carry out attribution assessments.

Figure 1 illustrates part of a fingerprint assessment of global temperature change at the surface during the late 20th century. The observed change in the latter half of the 20th century, shown by the black time series in the left panels, is larger than expected from just internal variability. Simulations driven only by natural forcings (yellow and blue lines in the upper left panel) fail to reproduce late 20th century global warming at the surface with a spatial pattern of change (upper right) completely different from the observed pattern of change (middle right). Simulations including both natural and human-caused forcings provide a much better representation of the time rate of change (lower left) and spatial pattern (lower right) of observed surface temperature change.

Both panels on the left show that computer models reproduce the naturally forced surface cooling observed for a year or two after major volcanic eruptions, such as occurred in 1982 and 1991. Natural forcing simulations capture the short-lived temperature changes following eruptions, but only the natural + human caused forcing simulations simulate the longer-lived warming trend.

The fingerprint patterns associated with individual forcings become easier to distinguish when more variables are considered in the assessment.

**Figure 1** (Left) Time series of global and annual-averaged surface temperature change from 1860 to 2010. The top left panel shows results from two ensemble of climate models driven with just natural forcings, shown as thin blue and yellow lines; ensemble average temperature changes are thick blue and red lines. Three different observed estimates are shown as black lines. The lower left panel shows simulations by the same models, but driven with both natural forcing and human-induced changes in greenhouse gases and aerosols. (Right) Spatial patterns of local surface temperature trends from 1951 to 2010. The upper panel shows the pattern of trends from a large ensemble of Coupled Model Intercomparison Project Phase 5 (CMIP5) simulations driven with just natural forcings. The bottom panel shows trends from a corresponding ensemble of simulations driven with natural + human forcings. The middle panel shows the pattern of observed trends from the Hadley Centre/Climatic Research Unit gridded surface temperature data set 4 (HadCRUT4) during this period.



Overall, Figure 1 shows that the pattern of observed temperature change is significantly different than the pattern of response to natural forcings alone. The simulated response to all forcings, including human-caused forcings, provides a good match to the observed changes at the surface. We cannot correctly simulate recent observed climate change without including the response to human-caused forcings, including greenhouse gases, stratospheric ozone, and aerosols. Natural causes of change are still at work in the climate system, but recent trends in temperature are largely attributable to human-caused forcing.

***When Will Human Influences on Climate Become Obvious on Local Scales?***

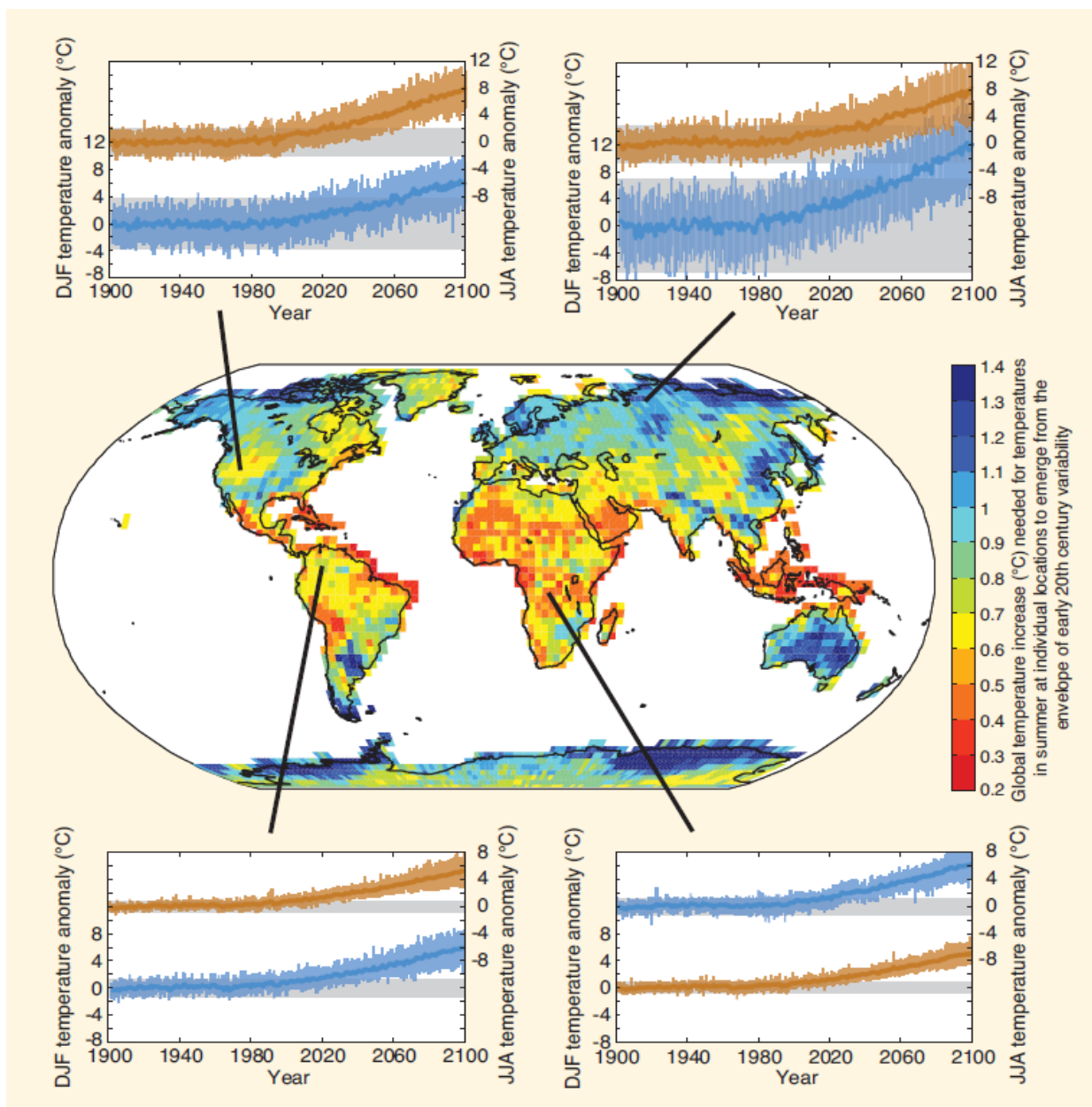
Human-caused warming is already becoming locally obvious on land in some tropical regions, especially during the warm part of the year. Warming should become obvious in middle latitudes—during summer at first—within the next several decades. The trend is expected to emerge more slowly there, especially during winter, because natural climate variability increases with distance from the equator and during the cold season. Temperature trends already detected in many regions have been attributed to human influence. Temperature-sensitive climate variables, such as Arctic sea ice, also show detected trends attributable to human influence.

Warming trends associated with global change are generally more evident in averages of global temperature than in time series of local temperature ('local' here refers generally to individual locations, or small regional averages). This is because most of the local variability of local climate is averaged away in the global mean. Multi-decadal warming trends detected in many regions are considered to be outside the range of trends one might expect from natural internal variability of the climate system, but such trends will only become obvious when the local mean climate emerges from the 'noise' of year-to-year variability. How quickly this happens depends on both the rate of the warming trend and the amount of local variability. Future warming trends cannot be predicted precisely, especially at local scales, so estimates of the future time of emergence of a warming trend cannot be made with precision.

In some tropical regions, the warming trend has already emerged from local variability (Figure 2). This happens more quickly **in the tropics** because there is less temperature variability there than in other parts of the globe. Projected warming may not emerge in middle latitudes until the mid-21st century—even though warming trends there are larger—because local temperature variability is substantially greater there than in the tropics. On a seasonal basis, local temperature variability tends to be smaller in summer than in winter. Warming therefore tends to emerge first in the warm part of the year, even in regions where the warming trend is larger in winter, such as in central Eurasia, Figure 2.

Variables other than land surface temperature, including some oceanic regions, also show rates of long-term change different from natural variability.

**Figure 2.** Time series of projected temperature change shown at four representative locations for summer (red curves, representing June, July and August at sites in the tropics and Northern Hemisphere or December, January and February in the Southern Hemisphere) and winter (blue curves). Each time series is surrounded by an envelope of projected changes (pink for the local warm season, blue for the local cold season) yielded by 24 different model simulations, emerging from a grey envelope of natural local variability simulated by the models using early 20th century conditions. The warming signal emerges first in the tropics during summer. The central map shows the global temperature increase (°C) needed for temperatures in summer at individual locations to emerge from the envelope of early 20th century variability. Note that warm colours denote the smallest needed temperature increase, hence earliest time of emergence. All calculations are based on Coupled Model Intercomparison Project Phase 5 (CMIP5) global climate model simulations forced by the Representative Concentration Pathway 8.5 (RCP8.5) emissions scenario. Envelopes of projected change and natural variability are defined as  $\pm 2$  standard deviations.



For example, Arctic sea ice extent is declining very rapidly, and already shows a human influence. On the other hand, local precipitation trends are very hard to detect because at most locations the variability in precipitation is quite large.

The probability of record-setting warm summer temperatures has increased throughout much of the Northern Hemisphere. High temperatures presently considered extreme are projected to become closer to the norm over the coming decades. The probabilities of other extreme events, including some cold spells, have lessened.

In the present climate, individual extreme weather events cannot be unambiguously ascribed to climate change, since such events could have happened in an unchanged climate. However the probability of occurrence of such events could have changed significantly at a particular location. Human-induced increases in greenhouse gases are estimated to have contributed substantially to the probability of some heatwaves. Similarly, climate model studies suggest that increased greenhouse gases have contributed to the observed intensification of heavy precipitation events found over parts of the Northern Hemisphere. However, the probability of many other extreme weather events may not have changed substantially. Therefore, it is incorrect to ascribe every new weather record to climate change.

The date of future emergence of projected warming trends also depends on local climate variability, which can temporarily increase or decrease temperatures. Furthermore, the projected local temperature curves shown in Figure 2 are based on multiple climate model simulations forced by the same assumed future emissions scenario. A different rate of atmospheric greenhouse gas accumulation would cause a different warming trend, so the spread of model warming projections (the coloured shading in Figure 2) would be wider if the figure included a spread of greenhouse gas emissions scenarios. The increase required for summer temperature change to emerge from 20th century local variability (regardless of the rate of change) is depicted on the central map in Figure 2.

A full answer to the question of when human influence on local climate will become obvious depends on the strength of evidence one considers sufficient to render something 'obvious'. The most convincing scientific evidence for the effect of climate change on local scales comes from analysing the global picture, and from the wealth of evidence from across the climate system linking many observed changes to human influence.

## **Greenhouse Gas Variations and Past Climate Responses<sup>5</sup>**

It is a fact that present-day (2011) concentrations of the atmospheric greenhouse gases (GHGs) carbon dioxide (CO<sub>2</sub>), methane (CH<sub>4</sub>) and nitrous oxide (N<sub>2</sub>O) exceed the range of concentrations recorded in ice cores during the past 800,000 years<sup>6</sup>. Past changes in atmospheric GHG concentrations can be determined with very high confidence from polar ice cores.

There is high confidence that changes in atmospheric CO<sub>2</sub> concentration play an important role in glacial–interglacial cycles. Although the primary driver of glacial–interglacial cycles lies in the seasonal and latitudinal distribution of incoming solar energy driven by changes in the geometry of the Earth’s orbit around the Sun (“orbital forcing”), reconstructions and simulations together show that the full magnitude of glacial–interglacial temperature and ice volume changes cannot be explained without accounting for changes in atmospheric CO<sub>2</sub> content and the associated climate feedbacks.

During the last deglaciation, it is very likely that global mean temperature increased by 3°C to 8°C. While the mean rate of global warming was very likely 0.3°C to 0.8°C per thousand years, two periods were marked by faster warming rates, likely between 1°C and 1.5°C per thousand years, although regionally and on shorter time scales higher rates may have occurred.

Global mean surface temperature was significantly above pre-industrial levels during several past periods characterised by high atmospheric CO<sub>2</sub> concentrations. During the mid-Pliocene (3.3 to 3.0 million years ago), atmospheric CO<sub>2</sub> concentrations between 350 ppm and 450 ppm occurred when global mean surface temperatures were 1.9°C to 3.6°C higher than for pre-industrial climate. During the Early Eocene (52 to 48 million years ago), atmospheric CO<sub>2</sub> concentrations exceeded ~1000 ppm when global mean surface temperatures were 9°C to 14°C higher than for pre-industrial conditions.

---

<sup>5</sup>AA. VV, 2013, “Information from Paleoclimate Archives. In: *Climate Change 2013: The Physical Science Basis. Contribution of Working Group I to the Fifth Assessment Report of the Intergovernmental Panel on Climate Change*”, Ch. 5, Cambridge University Press, Cambridge, United Kingdom and New York, NY, USA

<sup>6</sup> With very high confidence, the current rates of CO<sub>2</sub>, CH<sub>4</sub> and N<sub>2</sub>O rise in atmospheric concentrations and the associated radiative forcing are unprecedented with respect to the highest resolution ice core records of the last 22,000 years. There is medium confidence that the rate of change of the observed GHG rise is also unprecedented compared with the lower resolution records of the past 800,000 years

***Observed Recent Climate Change in the Context of Interglacial Climate Variability***

New temperature reconstructions and simulations of the warmest millennia of the last interglacial period (129,000 to 116,000 years ago) show that **global mean annual surface temperatures were never more than 2°C higher than pre-industrial**. High latitude surface temperature, averaged over several thousand years, was at least 2°C warmer than present. Greater warming at high latitudes, seasonally and annually, confirm the importance of cryosphere feedbacks to the seasonal orbital forcing. **During these periods, atmospheric GHG concentrations were close to the pre-industrial level.**

The annual mean surface warming since the 20th century has reversed long-term cooling trends of the past 5000 years in mid-to-high latitudes of the Northern Hemisphere (NH). New continental - and hemispheric-scale annual surface temperature reconstructions reveal multi-millennial cooling trends throughout the past 5000 years. The last mid-to-high latitude cooling trend persisted until the 19th century, and can be attributed with high confidence to orbital forcing, according to climate model simulations.

From reconstructions that the current (1980–2012) summer sea ice retreat was unprecedented and sea surface temperatures in the Arctic were anomalously high in the perspective of at least the last 1450 years. Lower than late 20th century summer Arctic sea ice cover is reconstructed and simulated for the period between 8000 and 6500 years ago in response to orbital forcing. Minima in NH extratropical glacier extent between 8000 and 6000 years ago were primarily due to high summer insolation (orbital forcing). **The current glacier retreat occurs within a context of orbital forcing that would be favourable for NH glacier growth.** If glaciers continue to reduce at current rates, most extratropical NH glaciers will shrink to their minimum extent, which existed between 8000 and 6000 years ago, within this century.

For average annual NH temperatures, the period 1983–2012 was very likely the warmest 30-year period of the last 800 years and likely the warmest 30-year period of the last 1400 years. Continental-scale surface temperature reconstructions show multi-decadal periods **during the Medieval Climate Anomaly (950 to 1250) that were in some regions as warm as in the mid-20th century and in others as warm as in the late 20th century.** With high confidence, these regional warm periods were not as synchronous across regions as the warming since the mid-20th century. Not only external orbital, solar and volcanic forcing, but also internal variability, contributed substantially to the spatial pattern and timing of surface temperature

changes between the Medieval Climate Anomaly and the Little Ice Age (1450 to 1850).

***Pre-Industrial non-anthropogenic perspective on Radiative Forcing Factors***

*Orbital Forcing.* The term is used to denote the incoming solar radiation changes originating from variations in the Earth's orbital parameters as well as changes in its axial tilt. Orbital forcing is well known from precise astronomical calculations for the past and future. Changes in eccentricity, longitude of perihelion (related to precession) and axial tilt (obliquity) predominantly affect the seasonal and latitudinal distribution and magnitude of solar energy received at the top of the atmosphere and the durations and intensities of local seasons.

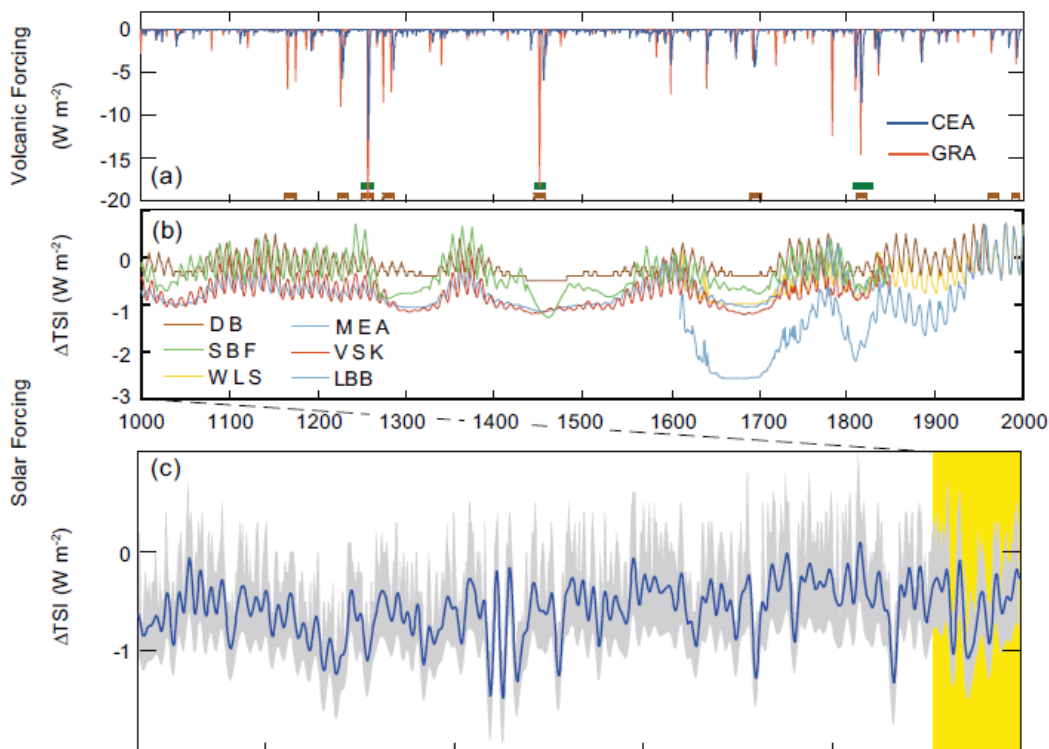
*Solar Forcing.* Solar irradiance models have been improved to explain better the instrumental measurements of total solar irradiance (TSI) and spectral (wavelength dependent) solar irradiance (SSI). Typical changes measured over an 11-year solar cycle are 0.1% for TSI and up to several percent for the ultraviolet (UV) part of SSI. Changes in TSI directly impact the Earth's surface, whereas changes in UV primarily affect the stratosphere, but can influence the tropospheric circulation. Most models attribute all TSI and SSI changes exclusively to magnetic phenomena at the solar surface (sunspots, faculae, magnetic network), neglecting any potential internal phenomena such as changes in energy transport. The balance of contrasting dark sunspots and bright faculae and magnetic network leads to a higher TSI value during solar cycle maxima and at most wavelengths. TSI and SSI are calculated by adding the radiative fluxes of all features plus the contribution from the magnetically inactive surface.

*Volcanic Forcing.* Volcanic activity affects global climate through the radiative impacts of atmospheric sulphate aerosols injected by volcanic eruptions. Quantifying volcanic forcing in the pre-satellite period is important for historical and last millennium climate simulations, climate sensitivity estimates and detection and attribution studies. Reconstructions of past volcanic forcing are based on sulphate deposition from multiple ice cores from Greenland and Antarctica, combined with atmospheric modelling of aerosol distribution and optical depth.

Two new reconstructions of the spatial distribution of volcanic aerosol optical depth have been generated using polar ice cores, spanning the last 1500 and 1200 years (Figure 5.1a). Although the relative size of eruptions for the past 700 years is generally consistent among these and earlier studies, they

differ in the absolute amplitude of peaks. There are also differences in the reconstructions of Icelandic eruptions, with an ongoing debate on the magnitude of stratospheric inputs for the 1783 Laki eruption;. The recurrence time of past large volcanic aerosol injections (eruptions changing the radiative forcing (RF) by more than  $1 \text{ W m}^{-2}$ ) varies from 3 to 121 years, with long-term mean value of 35 to 39 years, and only two or three periods of 100 years without such eruptions since 850.

**Figure 5.1** (a) Two reconstructions of *volcanic forcing* for the past 1000 years derived from ice core sulphate. Volcanic sulphate peaks identified from their isotopic composition as originating from the stratosphere are indicated by squares (green: Greenland; brown: Antarctica)  
 (b) Reconstructed *total solar irradiance* (TSI) anomalies back to the year 1000. Proxies of solar activity (e.g., sunspots, 10Be) are used to estimate the parameters of the models or directly TSI. For the years prior to 1600, the 11-year cycle has been added artificially to the original data with an amplitude proportional to the mean level of TSI.  
 (c) Reconstructed *TSI anomalies* (100-year low-pass filtered; grey shading: one standard deviation uncertainty range) for the past 9300 years. The yellow band indicates the past 1000 years shown in more details in (a) and (b). Anomalies are relative to the 1976–2006 mean value ( $1366.14 \text{ W m}^{-2}$ )

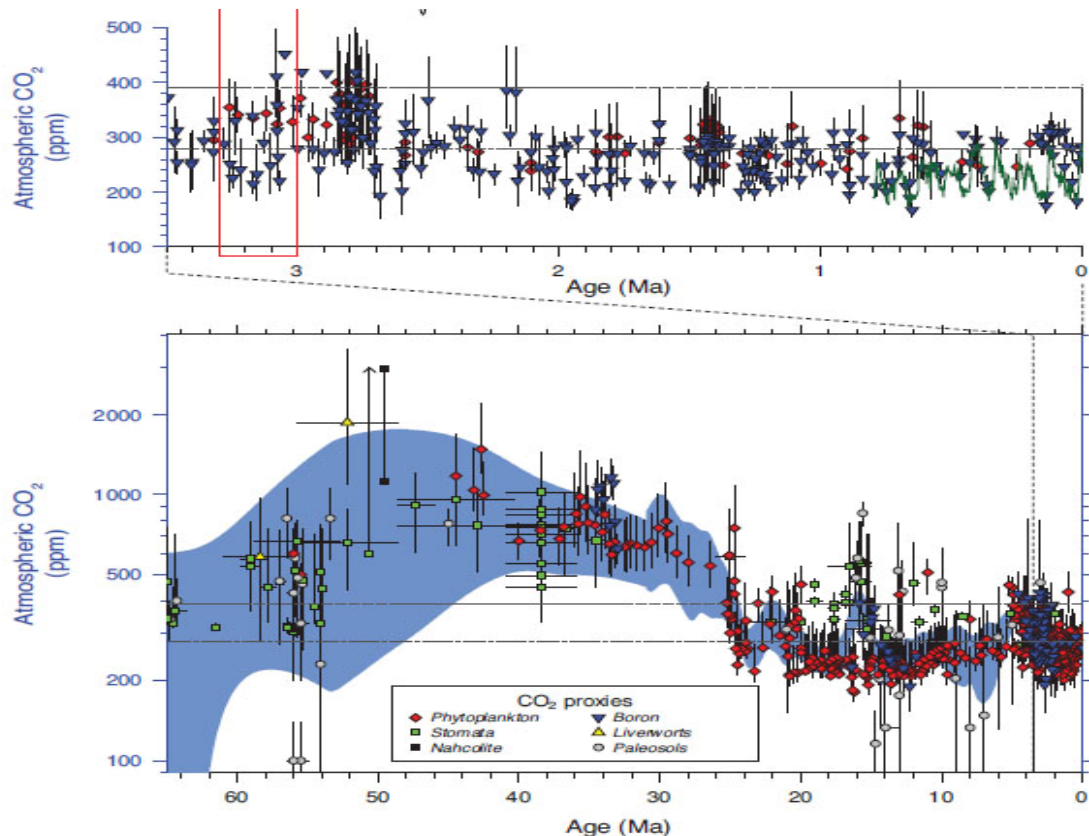


***Atmospheric Concentrations of Carbon Dioxide, Methane and Nitrous Oxide from Ice Cores***

Complementing instrumental data, air enclosed in polar ice provides a direct record of past atmospheric well-mixed greenhouse gas (WMGHG) concentrations. During the pre-industrial part of the last 7000 years, millennial (20 ppm CO<sub>2</sub>, 125 ppb CH<sub>4</sub>) and centennial variations (up to 10 ppm CO<sub>2</sub>, 40 ppb CH<sub>4</sub> and 10 ppb N<sub>2</sub>O) are recorded.

Long-term records have been extended to 800 kyr (Figure 5.. During the last 800 kyr, the pre-industrial ice core WMGHG concentrations stay within well-defined natural limits with maximum interglacial concentrations of approximately 300 ppm, 800 ppb and 300 ppb for CO<sub>2</sub>, CH<sub>4</sub> and N<sub>2</sub>O, respectively, and minimum glacial concentrations of approximately 180 ppm, 350 ppb, and 200 ppb. The new data show lower than pre-industrial (280 ppm) CO<sub>2</sub> concentrations during interglacial periods from 800 to 430 kyr. It is a fact that present-day (2011) concentrations of CO<sub>2</sub> (390.5 ppm), CH<sub>4</sub> (1803 ppb) and N<sub>2</sub>O (324 ppm) exceed the range of concentrations recorded in the ice core records during the past 800.000 years. The rate of change of the observed anthropogenic WMGHG rise and its RF is unprecedented with respect to the highest resolution ice core record back to 22 kyr for CO<sub>2</sub>, CH<sub>4</sub> and N<sub>2</sub>O. The rate of change of the observed anthropogenic WMGHG rise is also unprecedented with respect to the records of the past 800 kyr.

**Figure 5.2** Atmospheric carbon dioxide (CO<sub>2</sub>) measured from Antarctic ice cores (green line), and estimates of CO<sub>2</sub> from boron isotopes (d11B) in foraminifera in marine sediments (blue triangles), and phytoplankton alkenone-derived carbon isotope proxies (red diamonds), plotted with two standard deviation uncertainty. Present (2012) and pre-industrial CO<sub>2</sub> concentrations are indicated with long-dashed and short-dashed grey lines, respectively. (Bottom) Concentration of atmospheric CO<sub>2</sub> for the last 65 Ma is reconstructed from marine and terrestrial proxies. Individual proxy methods are colour-coded. The light blue shading is a one-standard deviation uncertainty band. Most of the data points for CO<sub>2</sub> proxies are based on duplicate and multiple analyses. The red box labelled MPWP represents the mid-Pliocene warm Period



*Maybe the Sun the Major Driver of Recent Changes in Climate?*

Total solar irradiance (TSI) is a measure of the total energy received from the sun at the top of the atmosphere. It varies over a wide range of time scales, from billions of years to just a few days, though variations have been relatively small over the past 140 years. Changes in solar irradiance are an important driver of climate variability along with volcanic emissions and anthropogenic factors. As such, they help explain the observed change in global surface temperatures during the instrumental period and over the last millennium. While solar variability may have had a discernible contribution to changes in global surface temperature in the early 20th century, it cannot explain the observed increase since TSI started to be measured directly by satellites in the late 1970s.

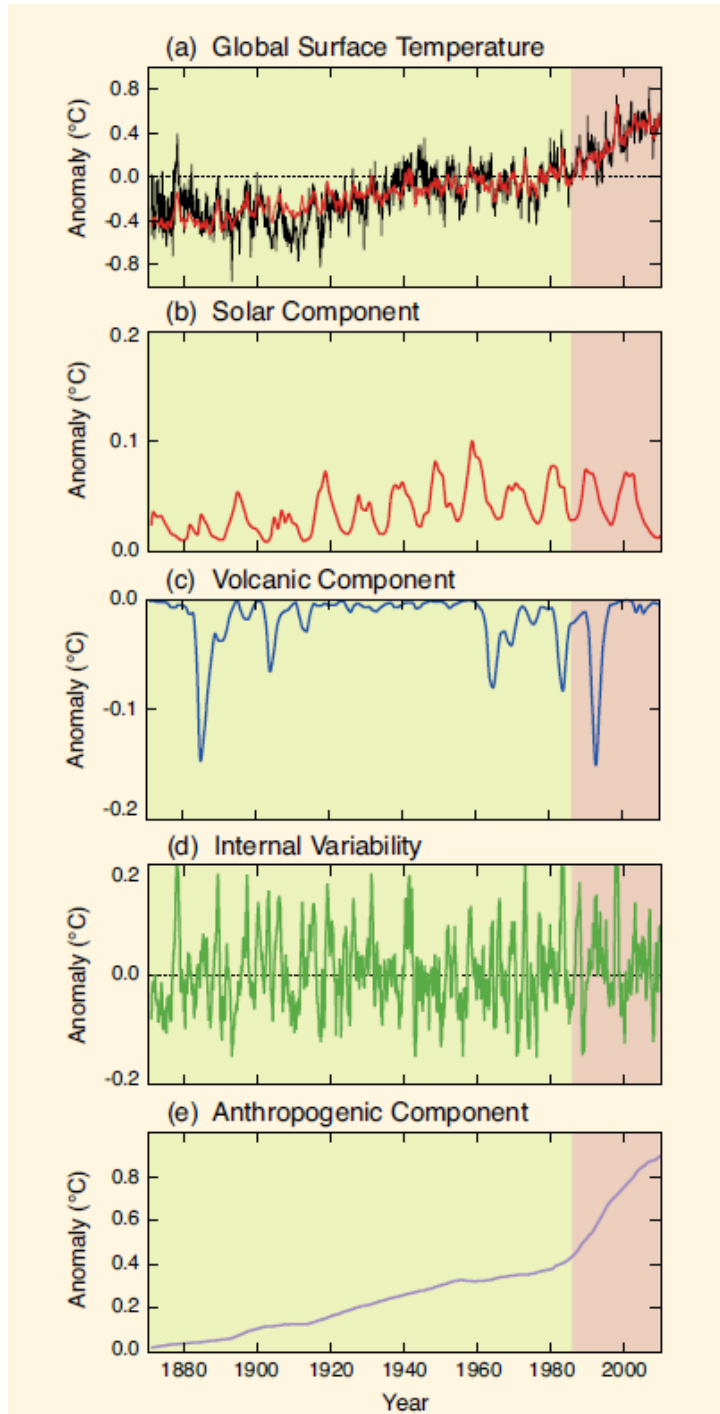


**Figure 3.** Global surface temperature anomalies from 1870 to 2010, and the natural (solar, volcanic, and internal) and anthropogenic factors that influence them. (a) Global surface temperature record (1870–2010) relative to the average global surface temperature for 1961–1990 (black line). A model of global surface temperature change (a: red line) produced using the sum of the impacts on temperature of natural (b, c, d) and anthropogenic factors (e). (b) Estimated temperature response to solar forcing. (c) Estimated temperature response to volcanic eruptions. (d) Estimated temperature variability due to internal variability, here related to the El Niño-Southern Oscillation. (e) Estimated temperature response to anthropogenic forcing, consisting of a warming component from greenhouse gases, and a cooling component from most aerosols.

The Sun's core is a massive nuclear fusion reactor that converts hydrogen into helium. This process produces energy that radiates throughout the solar system as electromagnetic radiation. The amount of energy striking the top of Earth's atmosphere varies depending on the generation and emission of electromagnetic energy by the Sun and on the Earth's orbital path around the Sun. Satellite-based instruments have directly measured TSI since 1978, and indicate that **on average,  $\sim 1361 \text{ W m}^{-2}$  reaches the top of the Earth's atmosphere**. Parts of the Earth's surface and air pollution and clouds in the atmosphere act as a mirror and reflect about 30% of this power back into space. Irradiance variations follow the roughly 11-year sunspot cycle: during the last cycles, TSI values fluctuated by an average of around 0.1%. For pre-satellite times, TSI variations have to be estimated from sunspot numbers (back to 1610), or from radioisotopes that are formed in the atmosphere, and archived in polar ice and tree rings.

How can solar variability<sup>7</sup> help explain the observed global surface temperature record back to 1870? To answer this question, it is important to understand that other climate drivers are involved, each producing characteristic patterns of regional climate responses. However, it is the combination of them all that causes the observed climate change. The relative contributions of these natural and anthropogenic factors change with time. Figure 3 illustrates those contributions based on a very simple calculation, in which the mean global surface temperature variation represents the sum of four components linearly related to **solar, volcanic, and anthropogenic forcing, and to internal variability**. Global surface temperature has increased by approximately 0.8°C from 1870 to 2010. However, this increase has not been uniform: at times, factors that cool the Earth's surface - volcanic eruptions, reduced solar activity, most anthropogenic aerosol emissions - have outweighed those factors that warm it, such as greenhouse gases, and the variability generated within the climate system has caused further fluctuations unrelated to external influences.

The **solar contribution** to the record of global surface temperature change is dominated by the 11-year solar cycle, which can **explain global temperature fluctuations up to approximately 0.1°C** between minima and maxima. A long-term increasing trend in solar activity in the early 20th century may

---

<sup>7</sup> Solar variability and volcanic eruptions are **natural factors**. **Anthropogenic factors**, on the other hand, include changes in the concentrations of greenhouse gases, and emissions of visible air pollution (aerosols) and other substances from human activities. **Internal variability** refers to fluctuations within the climate system, for example, due to weather variability or phenomena like the El Niño-Southern Oscillation

have augmented the warming recorded during this interval, together with internal variability, greenhouse gas increases and a hiatus in volcanism. However, it cannot explain the observed increase since the late 1970s, and there was even a slight decreasing trend of TSI from 1986 to 2008.

**Volcanic eruptions** contribute to global surface temperature change by episodically injecting aerosols into the atmosphere, which cool the Earth's surface. Large volcanic eruptions, such as the eruption of Mt. Pinatubo in 1991, can cool the surface by around 0.1°C to 0.3°C for up to three years.

The most important component of **internal climate variability** is the El Niño Southern Oscillation, which has a major effect on year-to-year variations of tropical and global mean temperature. Relatively high annual temperatures have been encountered during El Niño events, such as in 1997–1998.

The variability of observed global surface temperatures from 1870 to 2010 reflects the combined influences of natural solar, volcanic, internal factors, superimposed on the multi-decadal warming trend from anthropogenic factors. Prior to 1870, when anthropogenic emissions of greenhouse gases and aerosols were smaller, changes in solar and volcanic activity and internal variability played a more important role.

Solar minima lasting several decades have often been associated with cold conditions. However, these periods are often also affected by volcanic eruptions, making it difficult to quantify the solar contribution. At the regional scale, changes in solar activity have been related to changes in surface climate and atmospheric circulation. The mechanisms that amplify the regional effects of the relatively small fluctuations of TSI in the roughly 11-year solar cycle have little effect on global mean temperatures. Finally, a decrease in solar activity during the past solar minimum a few years ago (Figure 3b) raises the question of its future influence on climate. **Despite uncertainties in future solar activity, the effects of solar activity within the range of grand solar maxima and minima will be much smaller than the changes due to anthropogenic effects.**

### ***Temperature Variations During the Last 2000 Years***

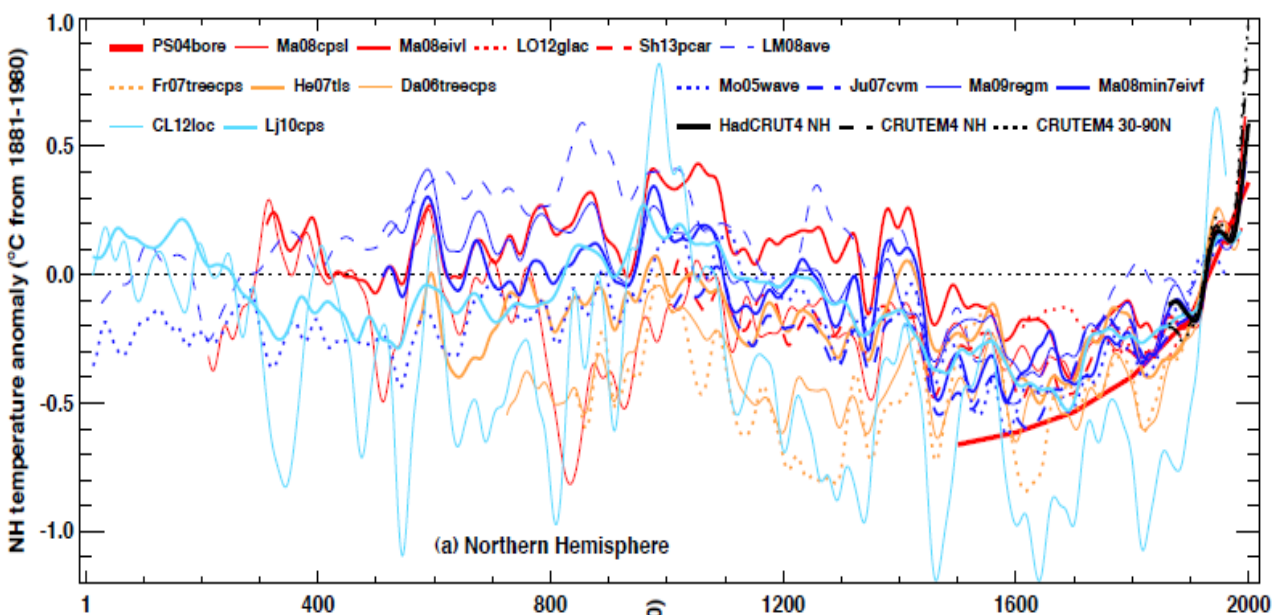
The last two millennia allow comparison of instrumental records with multi-decadal-to-centennial variability arising from external forcings and internal climate variability. New paleoclimate reconstruction efforts have provided further insights into the characteristics of the Medieval Climate Anomaly (MCA) and the Little Ice Age (LIA). The timing and spatial structure of the MCA and LIA are complex, with different reconstructions exhibiting warm

and cold conditions at different times for different regions and seasons. The median of the NH temperature reconstructions (Figure 5.7) indicates mostly warm conditions from about 950 to about 1250 and colder conditions from about 1450 to about 1850; these time intervals are chosen here to represent the MCA and the LIA, respectively.

The mean NH temperature of the last 30 or 50 years very likely exceeded any previous 30 - or 50 - year mean during the past 800 years. The timing of warm and cold periods is mostly consistent across reconstructions. Even accounting for these uncertainties, almost all reconstructions agree that each 30-year (50-year) period from 1200 to 1899 was very likely colder in the NH than the 1983–2012 (1963–2012) instrumental temperature.

NH reconstructions covering part or all of the first millennium suggest that **some earlier 50-year periods might have been as warm as the 1963–2012 mean instrumental temperature**, but the higher temperature of the last 30 years appear to be at least likely the warmest 30-year period in all reconstructions. Considering some caveats, there is confidence that **the last 30 years were likely the warmest 30-year period of the last 1400 years**.

**Figure 5.7** Reconstructed Northern Hemisphere global annual temperatures during the last 2000 years. Individual reconstructions are shown as indicated in the legends, grouped by colour according to their spatial representation (red: land-only all latitudes; orange: land-only extratropical latitudes; light blue: land and sea extra-tropical latitudes; dark blue: land and sea all latitudes) and instrumental temperatures shown in black, land and sea, and CRU Gridded Dataset of Global Historical Near-Surface Air TEMperature Anomalies Over Land version 4 (CRUTEM4) land-only). All series represent anomalies (°C) from the 1881–1980 mean (horizontal dashed line) and have been smoothed with a filter that reduces variations on time scales less than about 50 years



### *Past Interglacials Temperature Anomalies*

Interglacials of the past 800 kyr are characterized by different combinations of orbital forcing, atmospheric composition and climate responses. Documenting natural interglacial climate variability in the past provides a deeper understanding of the physical climate responses to orbital forcing. **The Last Interglacial** (LIG, 129.000 to 116.000 years ago) has more data and modelling studies for assessing regional and global temperature changes than earlier interglacials. **The current interglacial is the Holocene.**

Since 800 kyr, atmospheric **CO<sub>2</sub> concentrations during interglacials were systematically higher than during glacial periods.** Prior to ~430 kyr, ice cores from Antarctica record lower interglacial CO<sub>2</sub> concentrations than for the subsequent interglacial periods. While LIG WMGHG concentrations were similar to the pre-industrial Holocene values, orbital conditions were very different with larger latitudinal and seasonal insolation variations. Large eccentricity and the phasing of precession and obliquity during the LIG resulted in July 65°N **insolation peaking at ~126 kyr and staying above the Holocene maximum values from ~129 to 123 kyr.** The high obliquity contributed to small, but positive annual insolation anomalies at high latitudes in both hemispheres and negative anomalies at low latitudes. The highest and lowest interglacial temperatures occur in models when WMGHG concentrations and local insolation reinforce each other.

New quantitative data syntheses now allow estimation of maximum annual surface temperatures around the globe for the LIG. Overall, higher annual temperatures than pre-industrial are reconstructed for high latitudes of both hemispheres. At ~128 kyr, East Antarctic ice cores record early peak temperatures ~5°C above the present. Higher temperatures are derived for northern Eurasia and Alaska, with sites near the Arctic coast in Northeast Siberia indicating warming of more than 10°C as compared to late Holocene. Greenland warming of 8°C ± 4°C at 126 kyr is estimated from new Greenland ice cores.

Transient LIG simulations display peak NH summer warmth between 128 kyr and 125 kyr in response to orbital and WMGHG forcings. From data synthesis, **the LIG global mean annual surface temperature is estimated to be ~1°C to 2°C warmer than pre-industrial.** High latitude surface temperature, averaged over several thousand years, was at least 2°C warmer than present. In response to orbital forcing and WMGHG concentration changes, time slice simulations for 128 to 125 kyr exhibit global mean annual surface temperature changes of 0.0°C ± 0.5°C as

compared to pre-industrial. Peak global annual SST warming is estimated from data to be  $0.7^{\circ}\text{C} \pm 0.6^{\circ}\text{C}$ .

**Figure 5.6** Maximum annual surface temperatures anomalies for the Last Interglacial (LIG) as reconstructed from data and simulated by an ensemble of climate model experiments in response to orbital and well-mixed greenhouse gas (WMGHG) forcings. (a) Proxy data syntheses of annual surface temperature anomalies. An annual anomaly for each record was calculated as the average sea surface temperature (SST) of the 5-kyr period centred on the warmest temperature between 135 kyr and 118 kyr and then subtracting the average SST of the late Holocene (last 5 kyr). The annual temperature anomalies relative to 1961–1990 were calculated by averaging the LIG temperature estimates across the isotopic plateau in the marine and ice records and the period of maximum warmth in the terrestrial records. (b) Multi-model average of annual surface air temperature anomalies simulated for the LIG computed with respect to preindustrial. The results for the LIG are obtained from 16 simulations for 128 to 125 kyr conducted by 13 modelling groups. (c) Seasonal SST anomalies. Multi-model zonal averages are shown as solid line with shaded bands indicating two standard deviations. Plotted values are the respective seasonal multi-mean global average. Symbols are individual proxy records of seasonal SST anomalies. (d) Seasonal terrestrial surface temperature anomalies (SAT). In (c) and (d) JJA denotes June – July – August and DJF December – January – February, respectively.

